A Two-Tone Test Method for Continuous-Time Adaptive Equalizers

Dongwoo Hong*, Shadi Saberi**, Kwang-Ting (Tim) Cheng*, C. Patrick Yue*

University of California, Santa Barbara, CA, USA*
Carnegie Mellon University, Pittsburgh, PA, USA **

Abstract

This paper describes a novel test method for continuous-time adaptive equalizers. This technique applies a two-sinusoidal-tone signal as stimulus and includes an RMS detector for testing, which incurs no performance degradation and a very small area overhead. To validate the technique, we used a recently published adaptive equalizer as our test case and conducted both behavioral and transistor-level simulations. Simulation results demonstrate that the technique is effective in detecting defects in the equalizer, which might not be easily detected by the conventional eye-diagram method.

1. Introduction

With the increasing demand of higher bandwidth, the data rate of I/Os is approaching the tens of gigahertz range. While the continuing advancement of process technology enables an I/O chip to run at such frequencies, the bandwidth of the communication channels, including cables and legacy backplanes, has become the limiting factor.

The bandwidth limitation of the channel causes Inter-Symbol Interference (ISI). The channel loss due to the skin-effect and the dielectric loss causes signal dispersion. Thus, the signal is distorted by its own delayed versions. Various equalization techniques, which multiply the inverse response of the channel to flatten out the overall frequency response, have been developed to compensate for this channel effect. In addition, the channel characteristics may not be known in advance and might be time-variant [1]. To cope with such problems, several adaptation algorithms have also been developed to adjust the overall response depending on the channel conditions.

The equalizer can be implemented either in the transmitter or in the receiver. The implementation of the transmitter equalizer is relatively easier than that of the receiver equalizer because the required Finite Impulse Response (FIR) filter deals with the digital data at the transmitter side, rather than the received analog data at the receiver side [2, 3]. However, since channel information is not easily available at the transmitter, it is difficult to apply the adaptive technique at the transmitter.

The approaches of equalization at the receiver can be divided into two categories: discrete-time equalization and continuous-time equalization. A discrete-time equalizer, which is based on the FIR filter, can take advantage of various digital adaptive algorithms [4-7]. However, since equalization is based on the samples captured by the receiver's recovered clock, there exists a cross-dependence between the equalizer and the clock recovery circuit. As the data rate increases, the power consumption would increase dramatically due to the large number of taps implemented in this type of equalizers [8]. On the other hand, a continuous-time equalizer does not require a sampling clock and thus the equalizer would work independent of the clock recovery circuit. Continuous-time equalizers have been investigated for low power and high speed applications, and promising performance has been reported [8-13].

While equalizer design has been studied for a long time and a number of novel architectures have recently been developed, high-quality and cost-effective production test methods for these equalizers are not yet well developed. The most popular means of testing equalizers is to measure the eye-diagram using either an external scope or on-chip measurement circuitry [14]. These methods test the equalizer by simply comparing the eye-openings before and after the equalizer. However, the eye-opening results measured in the test environment would not match those in the real system if the channels in the test board and those in the real applications are different. In addition, measuring the eye-diagram in the multi-gigahertz range requires either expensive equipment for external measurement or a significant amount of internal circuitry for on-chip measurement. In [15], a cost-effective test method for adaptive equalizers is proposed. However, this technique has a limitation: it could not properly test the adaptation loop in the equalizer because the low frequency gain of the equalizer is programmed before testing.

In this paper, we propose a novel test method for a continuous-time adaptive equalizer. Our technique can cost-effectively test both the equalization filter and the adaptation loop. The advantages of the proposed technique are as follows: 1) the test stimuli can be easily generated and applied, which need not be stressed using different channels. 2) The test output is a DC signal and thus can be easily measured. 3) The extra on-chip circuitry needed for supporting the technique requires only a very small area overhead and does not result in any performance degradation.

978-3-9810801-2-4/DATE07 © 2007 EDAA

In the next section, we describe the basic operation of a continuous-time adaptive equalizer. Section 3 describes the proposed two-tone test method. Section 4 presents the experimental setup and results for the validation of the proposed technique. Section 5 concludes the paper and discusses future work.

2. Continuous-Time Adaptive Equalizer

The block diagram of a conventional continuous-time adaptive equalizer is shown in Fig. 1. The equalization filter either boosts the high-frequency components or attenuates the low-frequency components of the received input signal to compensate for high-frequency loss due to the channel. The adaptive servo loop, which adjusts the compensation gain of the equalization filter, determines the control voltage by comparing the input and the output signals of the comparator. In practice, it is difficult to design a comparator that can generate a clean waveform for comparisons at very high frequencies. Several new approaches for adaptation [11-13] have been proposed to address this problem. These new methods use the power spectrum derived from the output signal of the equalization filter for the adaptation, as shown in Fig. 2. Since the power spectrum of a random signal can be described by a sinc^2 function, the high-frequency loss can be detected by comparing the power densities of two different frequency ranges. Three different methods have been proposed to compare the power spectrum of the random signal. Two band-pass filters are used in [11] to compare the power of two specific frequencies. In [12], one low-pass filter and one high-pass filter are used to compare the power between the low-frequency and high-frequency portions of the signal. In [13], only one low-pass filter is used and the entire signal power is compared to the power of the low-frequency portion of the signal. Fig. 3 illustrates these three different power spectrum comparison architectures. Our proposed test method is applicable to the modified continuous-time adaptive equalizer (i.e. the type shown in Fig. 2) under any of these three architectures.

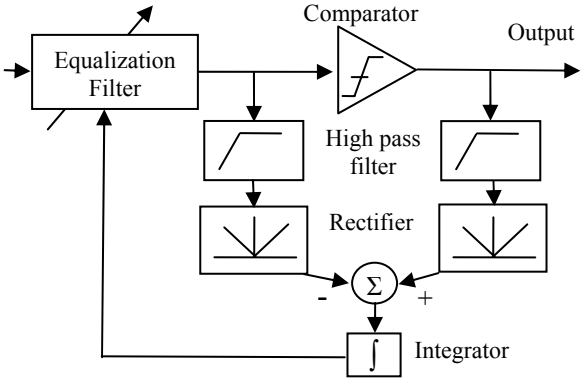

Fig. 1. Block diagram of a conventional continuous-time adaptive equalizer

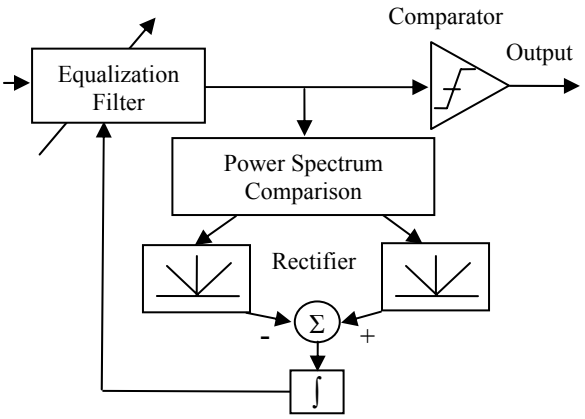

Fig. 2. Block diagram of a modified continuous-time adaptive equalizer

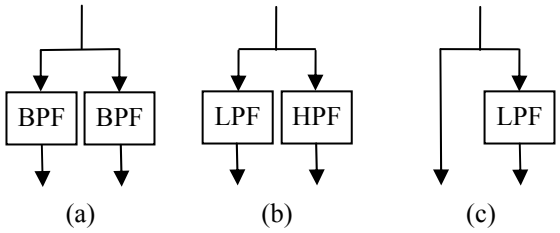

Fig. 3. Three different architectures for power spectrum comparison

3. Proposed Two-Tone Test Method

3.1. Description of the Test Method

The proposed test technique directly uses a two sinusoidal-tone signal as test stimulus instead of a data pattern stressed through the channel that has been commonly used for validating and characterizing the equalizers. The frequency for one of the two sinusoidal tones, denoted as f_L, falls within the stop-band region; the frequency of the other tone, denoted as f_H, falls within the pass-band region. Fig. 4 illustrates the frequency response of an adaptive equalizer that can compensate for the channel loss up to α_0 dB, and the frequency bands of two sinusoidal tones. In order to mimic the channel response, this technique repeatedly applies the two-tone signal and gradually varies the magnitude ratio of f_H and f_L. Specifically, we gradually increase the magnitude of f_L while fixing the magnitude of f_H. Such test stimuli mimic different relative losses of the high-frequency components caused by the channel. While this could also be accomplished by gradually reducing the magnitude of f_H and fixing the magnitude of f_L, it is much easier in practical implementations to adjust the magnitude of the low-frequency component.

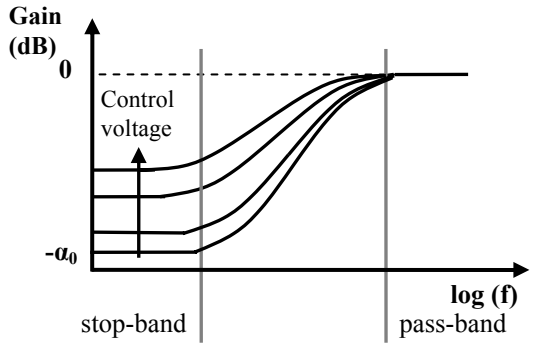

Fig. 4. Frequency response of an adaptive equalizer

With the test stimuli, we measure the Root Mean Square (RMS) value at the output of the equalizer. The adaptive servo loop attempts to maintain the ratio of f_L to f_H to the expected level based on the sinc^2 function. Thus, as illustrated in Fig. 5(a), if the test stimulus's f_L magnitude is within the range of R1 and, therefore, the magnitude ratio of f_L to f_H is within the range of the equalizer's maximum compensation gain (i.e. $G_{EQ\_Max} = 10^{\alpha_0/20}$), the RMS value of the equalizer output should be a constant. When the magnitude of f_L is increased to the point that the magnitude ratio of f_L to f_H exceeds the maximum compensation gain of the equalizer (as indicated in Fig. 5(a) where the magnitude of f_L is in the range of R2), the RMS value at the equalizer output will start to increase. Fig. 5(b) illustrates how the RMS value at the equalizer output would vary with respect to the magnitude of the f_L (with a fixed magnitude of f_H). Therefore, we can test the equalizer's maximum compensation gain, which is a key design specification of the equalizer, by identifying the magnitude of f_L when the RMS value starts to deviate from the expected value, denoted as A_{fL_Max} in Fig. 5(b). The adaptive loop also can be tested by the constant RMS values up to the A_{fL_Max}. Note that the conventional eye-diagram method may not easily test these specifications because: 1) designing the test board channel to exactly match the expected high-frequency loss is difficult. 2) It requires a number of different channel lengths for testing the adaptive loop, and this may not be feasible for production testing.

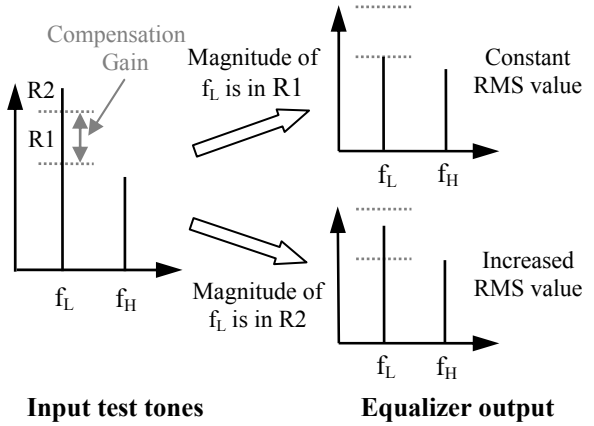

(a) Magnitude variations of two sinusoidal signals

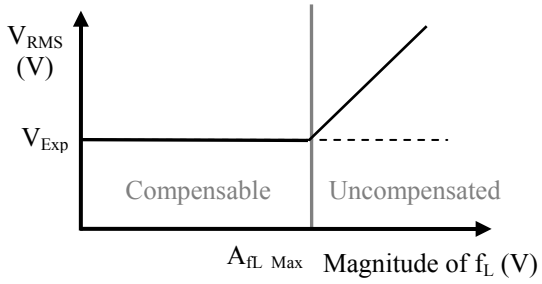

(b) Output RMS value vs f_L's magnitude

Fig. 5. Illustration of the two-tone test technique

There are two possible locations for measuring the RMS value: either node A or node B (denoted in Fig. 6). The RMS measurement at node A would be the combined RMS value of f_L and f_H which is the same as the equalizer's output RMS value. The RMS measurement at node B would also result in a similar curve as that seen in Fig. 5(b) because the magnitude of f_H remains constant and only the magnitude of f_L varies.

3.2. Implementation of the Test Method

We applied the proposed test technique to a continuous-time adaptive equalizer recently presented in [13,17] whose block diagram is shown in Fig. 6. It uses a passive equalization filter whose control voltage is adjusted by the servo loop based on the power spectrum of the data (i.e. the type shown in Fig. 3(c)). For this type of equalizer, since the rectifiers already exist in the architecture, we only need to add an LPF to implement the RMS detector.

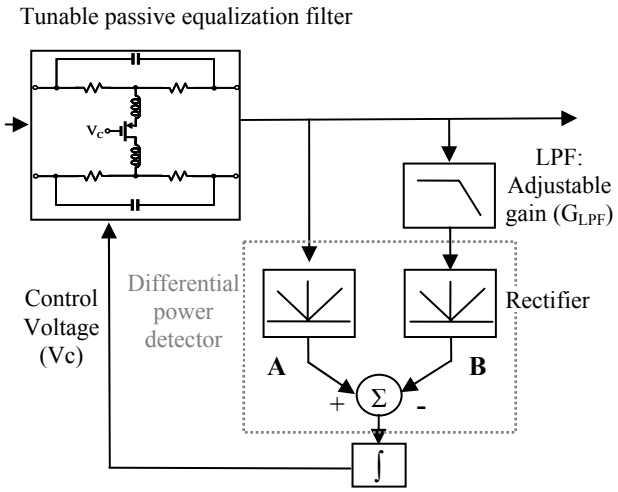

Fig. 6. Block diagram of the adaptive equalizer

We denote f_L's magnitude after the equalization filter as A_{fL_Out} and f_H's magnitude after the equalization filter as A_{fH}. The adaptive servo loop attempts to make the power of the two paths equal. That is:

$$A_{fL\_Out}^2 \times G_{LPF}{}^2 = A_{fL\_Out}^2 + A_{fH}^2$$

Therefore, the expected ratio of A_{fH} to A_{fL_Out}, denoted by K_{Exp}, becomes:

$$K_{Exp} = \frac{A_{fH}}{A_{fL\_Out}} = \sqrt{G_{LPF}^2 - 1} \qquad (1)$$

where G_{LPF} is the LPF voltage gain (see Fig. 6).

Note that the f_H's magnitude before the equalization filter is the same as A_{fH} because the gain of the equalization filter is close to 1 in the pass-band. If we denote f_L's magnitude before the equalization filter as A_{fL_In}, we can then derive the expected RMS value (V_{Exp}) as follows:

1) When A_{fL_In} is in R1 (as shown in Fig. 5(a))

The RMS values at node A and node B would be:

$$V_{RMS(A)} = \sqrt{(A_{fL\_Out}^2 + A_{fH}^2)/2} = G_{LPF} A_{fH} / \sqrt{2G_{LPF}^2 - 2}$$

$$V_{RMS(B)} = G_{LPF} A_{fL\_Out} / \sqrt{2} = G_{LPF} A_{fH} / \sqrt{2G_{LPF}^2 - 2}$$

Note that we modify both of the equations with respect to A_{fH} using Equation (1). Then, the RMS values for both cases are the same as expected because A_{fH} is a constant. Therefore, the expected RMS value would be

$$V_{Exp} = G_{LPF} A_{fH} / \sqrt{2G_{LPF}^2 - 2} \qquad (2)$$

2) When A_{fL_In} is in R2 (as shown in Fig. 5(a))

The RMS value at A and B would be:

$$V_{RMS(A)} = \sqrt{(A_{fL\_Out}^2 + A_{fH}^2)/2} = \frac{\sqrt{A_{fL\_In}^2 + A_{fH}^2 G_{EQ\_Mzx}^2}}{\sqrt{2} G_{EQ\_Max}}$$

$$V_{RMS(B)} = G_{LPF} A_{fL\_Out} / \sqrt{2} = \frac{G_{LPF} A_{fL\_In}}{\sqrt{2} G_{EQ\_Max}} \qquad (3)$$

In this region, since the equalizer cannot fully attenuate the low-frequency component to the desired level, the RMS value would be higher than the expected level and would thus increase as A_{fL_In} increases. However, the increasing rate would be different for these two locations. The increasing rate of the RMS value measured at B would be greater because it is multiplied by G_{LPF} as shown in Equation (3).

The magnitude of f_L at which the RMS value starts to deviate from the expected value can also be represented using Equation (1):

$$A_{fL\_Max} = \frac{A_{fH}}{K_{Exp}} \cdot G_{EQ\_Max} \qquad (4)$$

Therefore, by measuring the A_{fL_Max}, we can test both the equalization filter and the adaptive servo loop. Any defects and/or errors that cause variations to G_{EQ_Max} and K_{Exp} would be detected.

4. Experimental results

To validate the proposed technique, we conducted both behavioral-level simulation using Matlab and transistor-level simulation using Cadence Spectre. The design parameters of the equalizer used for the experiment are:

- G_{EQ_Max} = 17 dB = 7
- G_{LPF} = 3.1
- f_H = 5 GHz and A_{fH} = 80 mV
- f_L = 100 MHz and A_{fL_In} = 80 ~ 340 mV

Based on these parameters, the V_{Exp} and A_{fL_Max} can be calculated using Equations (3) and (4):

- V_{RMS} = 60 mV
- A_{fL_Max} = 191 mV

4.1. Matlab Simulation Results

Two sinusoidal signals are injected into the behavioral model of the equalizer and the RMS values are measured at A and B. For each location, the simulation is repeated by gradually increasing the magnitude of the low-frequency component ($A_{fL\ In}$).

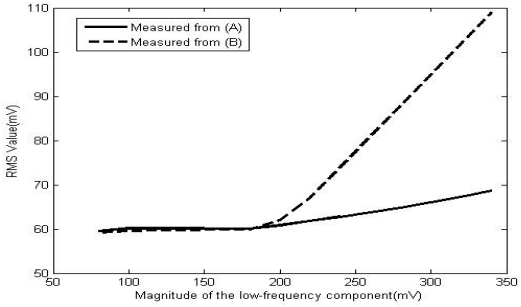

Fig. 7. Matlab simulation results

Fig. 7 shows the simulation results for both cases. The RMS values for both cases are constant up to 180mV and start to increase around 200mV. The expected A_{fL_Max} shown previously is about 190mV. As the step size of A_{fL_In} in our experiment was 20mV, the RMS value increases only slightly at 200mV but increases rapidly starting from 220mV. This result indicates that the proposed method could indeed identify the device's A_{fL_Max} fairly accurately. However, the increasing rate for measurement at A is small - the difference of the RMS values between steps is only a few mV. This difference would be too small to be detected in real applications,

particularly in the presence of various noise sources. For our test case, the expected ratio of A_{fH} to A_{fL_Out} is about 3. Therefore, the RMS value of A_{fH}, which is constant, would be significantly larger than that of A_{fL_Out}. Thus there would be a small variation to the total RMS value measured at A. Based on this observation, we implemented the RMS detector at B for transistor-level simulation. However, for designs with a small ratio of A_{fH} to A_{fL_Out}, the RMS detector placed at A could be a viable solution, too.

We injected a couple of parametric faults to the equalizer for simulation and examined the RMS value at B to check whether the faults are detectable by this technique. Specifically, we change the maximum compensation gain of the equalizer to (1) 13dB and (2) 10dB from 17dB. Note that defects/errors that cause the equalizer to malfunction would cause changes to its maximum compensation gains.

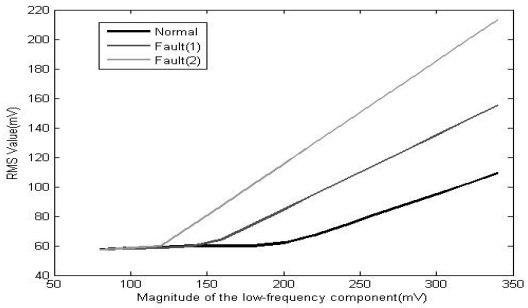

Fig. 8. Fault simulation results

Based on Equation (4), if the maximum compensation gain is reduced, the RMS value would start deviating from the expected value at a lower magnitude. Fig. 8 shows the simulation results of the three cases (fault-free circuit and faulty circuits (1) and (2)). The maximum compensation gain's variation can be easily identified by the detection of the change to A_{fL_Max}.

4.2. Transistor-Level Simulation Results

The continuous-time adaptive equalizer shown in Fig. 6 has been designed in a 0.13-µm CMOS process. The design details of the tunable passive equalization filter was reported in [13]. The die photo and the measured filter response are shown in Fig. 9. The filter can compensate for a loss up to 17dB at 5 GHz with a control voltage ranging from 0.1 to 0.6 V.

The RMS detector is implemented inside the differential power detector in the servo loop (see Fig. 6). We reuse the rectifier in the servo loop and only add a simple RC low-pass filter at the output of the rectifier. To avoid degrading the servo loop's performance, a current mirror is used to copy the output of the rectifier. Fig. 10 shows the schematic of the differential power detector and the RMS detector.

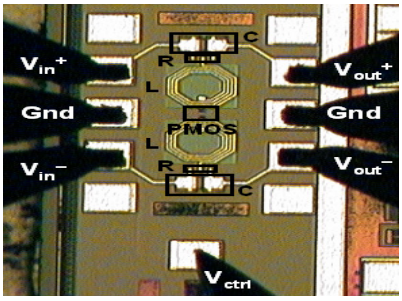

(a) Chip micrograph of the 0.13-µm filter prototype.

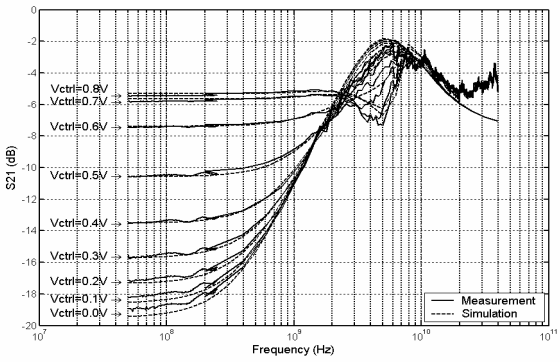

(b) Measurement vs. simulation results of the filter's differential S_{21}.

Fig. 9. Die photo and the filter response

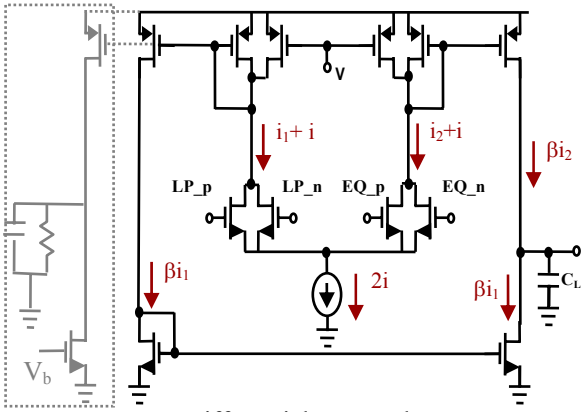

Fig. 10. Schematic of the differential power detector with RMS detector

Fig. 11(a) shows the RMS values measured before the simple RC LPF. Fig. 11(b) shows the DC output of the RMS detector. For both figures, we compare the nominal case with two defective cases. For the defective cases, the gain of the servo loop's LPF (G_{LPF}) was changed to 3.75 (Fault A) and 4.5 (Fault B), respectively. This in turn also results in a different A_{fL_Max}. The RMS values start to deviate at a lower A_{fL_In} for the defective cases as expected from Equation (4). Therefore, any variation in the adaptive loop also can be easily identified by the change to A_{fL_Max}.

Compared to the Matlab simulation results, the transistor-level simulation shows that the output RMS values are not constant, even within the equalizer's compensation gain range. This is because the gain of the equalization filter at 5GHz slightly varies depending on the control voltage, which in turn contributes to the variation in the expected RMS value. However, since the difference in slope between the two regions is obvious, we could still clearly identify A_{fL_Max}.

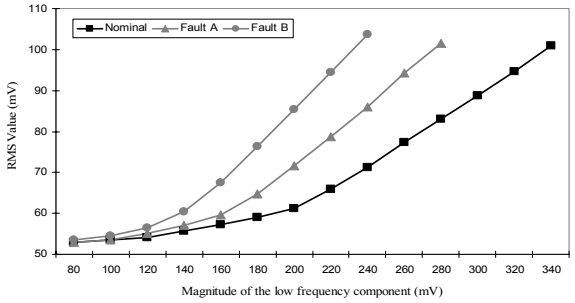

(a) Measured RMS value before the RC LPF

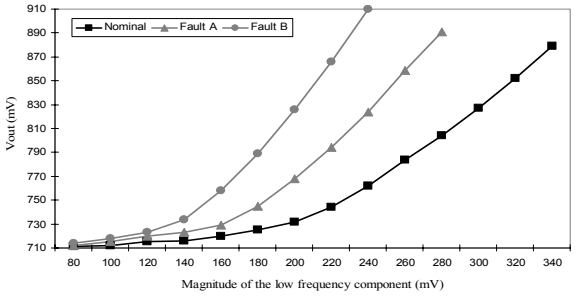

(b) DC output of the RMS detector

Fig. 11. Spectre simulation results

5. Conclusion

We propose an efficient method for testing the continuous-time adaptive equalizer that uses a simple two-tone signal as a test stimulus and an RMS detector for on-chip measurement. This technique can detect defects either in the equalization filter or in the adaptive servo loop that might not be easily detectable by the conventional eye-diagram method. We validated the idea by simulation using a recently proposed continuous-time adaptive equalizer. The behavioral and the transistor-level simulation results demonstrate the validity of our test technique.

In this paper, we focus the discussion on testing a stand-alone continuous-time adaptive equalizer. This technique could be extended for the adaptive equalizers built in a high-speed transceiver. For such an extension, the high-frequency sinusoidal component would be replaced by a clock-like pattern generated by the transmitter in the loop-back test mode that has been the most popular means of testing high-speed transceivers [15,16]. In addition, the low-frequency sinusoidal component would be added from external equipment. To further remove the need for external equipment in the loop-back test, we are investigating a cost-effective, on-chip low-frequency sinusoidal noise injection method to support this technique.

6. References

[1] J. Zerbe, "Comparison of adaptive and non-adaptive equalization methods in high-performance backplanes," *DesignCon*, 2005.

[2] J. Liu and X. Lin, "Equalization in High-Speed Communication Systems," *IEEE Circuits and Systems Magazine*, Second quarter 2004, pp. 4-17.

[3] W.J. Dally and J. Poulton, "Transmitter equalization for 4-Gbps signaling," *IEEE Micro.*, Jan/Feb 1997, pp. 48-56.

[4] J.E. Jaussi et al, "An 8Gb/s Source-Synchronous I/O Link with Adaptive Receiver Equalization, Offset Cancellation and clock De-Skew," *IEEE Journal of Solid-State Circuits*, Vol. 40, No. 1, January 2005, pp. 80-85.

[5] T. Beukema et al, "A 6.4Gb/s CMOS SerDes Core with Feed-Forward and Decision-Feedback Equalization," *IEEE Journal of Solid-State Circuits*, Vol. 40, No. 12, December 2005, pp. 2633-2645.

[6] J. Kim et al, "A Four-Channel 3.125-Gb/s/ch CMOS Serial-Link Transceiver with a Mixed-Mode Adaptive Equalizer," *IEEE Journal of Solid-State Circuits*, Vol. 40, No. 2, February 2005, pp. 462-471

[7] V. Stojanovic et al, "Autonomous Dual-Mode (PAM2/4) Serial Link Transceiver with Adaptive Equalization and Data Recovery," *IEEE Journal of Solid-State Circuits*, Vol. 40, No. 4, April 2005, pp. 1012-1026.

[8] R. Sun et al, "A Low-Power, 20-Gb/s Continuous-Time Adaptive Passive Equalizer," *IEEE Int. Circuit and Systems,* , September 2005, pp. 920-923.

[9] J. Choi et al, "A 0.18-um CMOS 3.5-Gb/s Continuous-Time Adaptive Cable Equalizer Using Enhanced Low-Frequency Gain Control Method," *IEEE Journal of Solid-State Circuits*, Vol. 39, No. 3, March 2004, pp. 419-425.

[10] G. Ahang et al, "A BiCMOS 10Gb/s Adaptive Cable Equalizer," *IEEE Int. Solid-State Circuits Conf.*, February 2004, pp. 92-93.

[11] Maxim Integrated Products, "Designing a simple, wide-band and low-power equalizer for FR4 copper link," *DesignCon*, 2003.

[12] J. Lee, "A 20-Gb/s Adaptive Equalizer in 0.13um CMOS Technology," *IEEE Int. Solid-State Circuits Conf.*, February 2006, pp. 92-93.

[13] R. Sun et al., "A Tunable Passive Filter for Low-Power High-Speed Equalizers," *IEEE VLSI Circuit Symposium*, June 2006.

[14] J.E. Jaussi et al, "An 8Gb/s Simultaneous Bidirectional Link with On-Die Waveform Capture," *IEEE Journal of Solid-State Circuits*, Vol. 38, No. 12, December 2003, pp. 2111-2120.

[15] I. Robertson, "Testing High-Speed, Large Scale Implementation of SerDes I/Os on Chips Used in Throughput Computing Systems," In Proc. of International Test Conference, 2005, pp 1-8.

[16] M. Tripp et al, "Elimination of Traditional Functional Testing of Interface Timings at Intel," In Proc. of International Test Conference, 2003, pp 1014-1022.

[17] R. Sun, "A Low-Power, 20-Gb/s Continuous-Time Adaptive Passive Equalizer," MS thesis, Carnegie Mellon University, December 2005.